ISSN 0020-1685, Inorganic Materials, 2008, Vol. 44, No. 9, pp. 965–970. © Pleiades Publishing, Ltd., 2008.
Original Russian Text © T.P. Smirnova, V.V. Kaichev, L.V. Yakovkina, V.I. Kosyakov, S.A. Beloshapkin, F.A. Kuznetsov, M.S. Lebedev, V.A. Gritsenko, 2008, published in Neorganicheskie Materialy, 2008, Vol. 44, No. 9, pp. 1086–1092.

Composition and Structure of Hafnia Films on Silicon

T. P. Smirnova[a], V. V. Kaichev[b], L. V. Yakovkina[a], V. I. Kosyakov[a], S. A. Beloshapkin[c], F. A. Kuznetsov[a], M. S. Lebedev[a], and V. A. Gritsenko[d]

[a] *Nikolaev Institute of Inorganic Chemistry, Siberian Division, Russian Academy of Sciences, pr. Akademika Lavrent'eva 3, Novosibirsk, 630090 Russia*

[b] *Boreskov Institute of Catalysis, Siberian Division, Russian Academy of Sciences, pr. Akademika Lavrent'eva 5, Novosibirsk, 630090 Russia*

[c] *Materials and Surface Science Institute, University of Limerick, Limerick, Ireland*

[d] *Institute of Semiconductor Physics, Siberian Division, Russian Academy of Sciences, pr. Akademika Lavrent'eva 13, Novosibirsk, 630090 Russia*

e-mail: smirn@che.nsk.su

Received October 11, 2006; in final form, June 22, 2007

Abstract—Ellipsometry, electron microscopy, and x-ray photoelectron spectroscopy data indicate that, during HfO_2 deposition onto silicon, the native oxide reacts with the HfO_2 deposit to form an amorphous intermediate layer which differs in refractive index (≃1.6) from both HfO_2 (1.9–2.0) and SiO_2 (1.46). Thermodynamic analysis of the Si–SiO_2–HfO_2–Hf system shows that Si is in equilibrium with Si/HfO_{2-y} only at low oxygen pressures. Starting at a certain oxygen pressure (equivalent to the formation of a native oxide layer), the equilibrium phase assemblage is $Si/HfSiO_4/HfO_{2-y}$.

DOI: 10.1134/S0020168508090124

INTRODUCTION

Advances in Si/SiO_2-based microchip integration technologies have almost reached their limit [1, 2]. For example, at a component size of 90 nm, the gate insulator thickness in planar field-effect transistors is 1.2 nm, i.e., about five SiO_2 monolayers. The key to further miniaturization of transistors lies in replacing silica by materials with a larger dielectric constant, so-called high-*k* dielectrics.

To ensure thermodynamic stability of silicon/insulator systems, the gate insulator must be nonreactive with silicon, and its constituent components when present as impurities should produce no undesirable levels in the band gap of the insulator layer. For a composite to be mechanically stable, its components must adhere well to one another and be close in thermal expansion. Moreover, the insulator should undergo no phase transitions between room temperature and the film growth temperature. Thermodynamic evaluation, supported by experimental data on the growth and dielectric properties of films, suggests that HfO_2 is potentially attractive as a microelectronic material [3, 4]. At the same time, increasing the number of components in a chemical system may result in special features that have not been encountered in the conventional Si/SiO_2 technology.

In this paper, we report the chemical and crystal structures of HfO_2 films grown on single-crystal silicon substrates.

EXPERIMENTAL

HfO_2 films 15–50 nm in thickness, with n = 1.9–2.0, were grown by metalorganic chemical vapor deposition (MOCVD) using hafnium dipivaloylmethanate, $Hf(dpm)_4$ (dpm = $C(CH_3)_3COCHCO(CH_3)_3$), as the precursor. The experimental arrangement and growth procedure were described in detail elsewhere [4].

We studied the chemical structure of two series of samples. Samples A were prepared on silicon substrates oxidized in oxygen at 900°C to produce an SiO_2 layer ≃20 nm thick. Next, a 30-nm-thick HfO_2 layer was deposited onto the silica. Samples B were produced by depositing HfO_2 onto silicon substrates covered with an oxide layer ≃5 nm thick. The substrate temperature during film growth was 650°C. The samples were annealed at 800°C for 1 h.

The thickness and refractive index of the films were determined by ellipsometry (LEF-3M, λ = 632.8 nm). Measurements were made at seven angles of incidence. The inverse ellipsometric problem was solved in one-, two-, and three-layer models using the NELM program. To determine initial approximations, calculations were made for the seven pairs of ψ and Δ in a one-layer nonabsorbing film model using nomogram analysis with the NOMOGR program.

The chemical structure of the films was probed by x-ray photoelectron spectroscopy (XPS). XPS spectra were measured on a VG ESCALAB HP spectrometer, using an Al K_α x-ray source ($h\nu$ = 1486.6 eV). As bind-

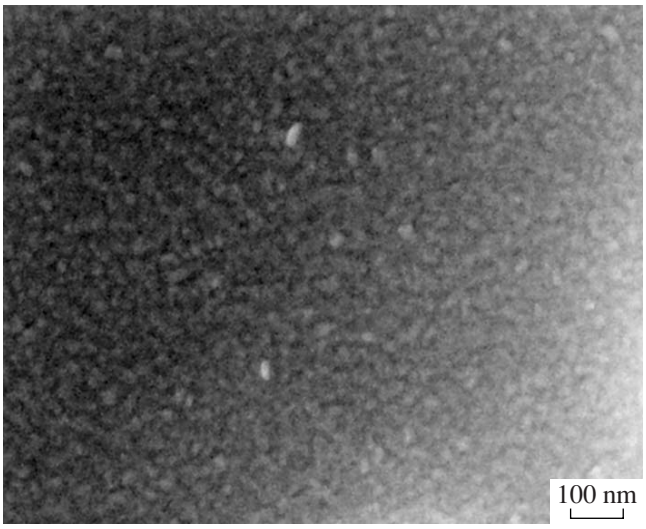

Fig. 1. Surface SEM image of an HfO_2 film grown at 650°C.

ing energy (E_b) scale references, we used the Au $4f_{7/2}$ (84.0 eV) and Cu $2p_{3/2}$ (932.67 eV) core levels arising from the surfaces of gold and copper foils, respectively. The sample composition in the probed zone (2- to 3-nm depth) was determined from integrated XPS intensities using relative sensitivity factors [5]. To gain more detailed information, the XPS spectra were decomposed into individual components. After subtracting the background by the Shirley method, the experimental spectrum was decomposed into a number of components corresponding to core-electron photoemission from atoms in different chemical environments. Composition–depth profiles were obtained using 3-keV Ar^+ ion milling at a current density of ≃30 μA/cm^2. The material removal rate was ≃1–2 nm/min [5].

X-ray diffraction (XRD) measurements were performed on a DRON-SEIFERT-RM4 diffractometer (CuK_α radiation, diffracted-beam graphite monochromator, scintillation detector, multichannel pulse amplitude analyzer). XRD patterns were collected in the step-scan mode in the 2θ range 5° – 60°. Polycrystalline silicon (a = 5.4309 Å) was used as an external standard. Phases were identified using earlier data [6, 7]. The surface morphology of the films was examined by scanning electron microscopy (SEM) on a JEOL JSM-6700F. Variations in film structure with depth were investigated by high-resolution transmission electron microscopy (HRTEM) on a JEOL JEM-2010 operated at an accelerating voltage of 200 keV. Cross-sectional specimens were prepared by focused ion beam milling (FEI FIB-200) [8]. To protect the HfO_2 layer during the FIB milling process, a carbon layer was deposited on the film surface.

RESULTS AND DISCUSSION

Structure of the films. Figure 1 is a surface SEM image of film B, grown at 650°C. The film is seen to be homogeneous and to consist of grains typically several nanometers to tens of nanometers in size. More detailed information about the microstructure of the films was obtained by HRTEM (Fig. 2). The dark-field cross-sectional TEM image in Fig. 2a shows well-resolved crystallites in the HfO_2 film, ranging in size from 5 to 20 nm. The selected area diffraction (SAD) pattern in the inset of Fig. 2 indicates good crystallinity of the hafnia film. The bright-field TEM image of the HfO_2/Si interface

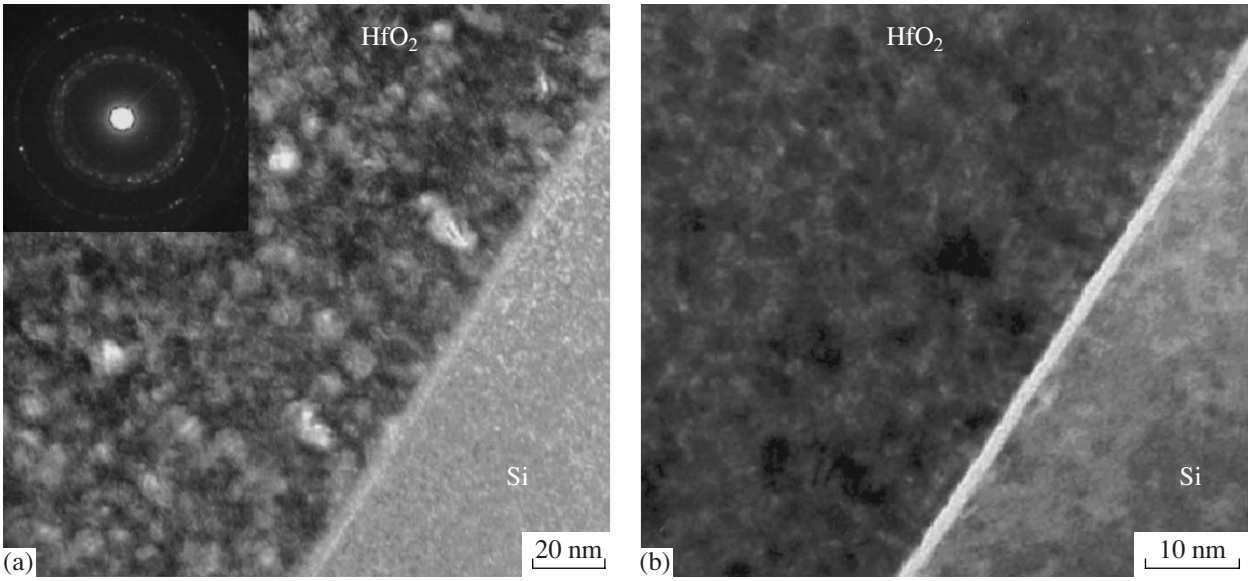

Fig. 2. (a) Dark- and (b) bright-field cross-sectional TEM images of sample B. Inset: SAD pattern.

shows a well-defined amorphous layer ≃5 nm in thickness (presumably, SiO_2 or a hafnium silicate).

According to XRD data, the crystalline phase was monoclinic HfO_2 (Fig. 3). Annealing at 800°C for 1 h caused the XRD peaks of the films to notably narrow, which may be considered evidence for ordering of the monoclinic structure (or an increase in crystallite size).

Ellipsometry data also indicated that the HfO_2 films had an inhomogeneous structure. Calculations in a three-layer model showed that samples A consisted of three layers with refractive indices of 1.97 (HfO_2), 1.62 (presumably, $Hf_xSi_yO_z$), and 1.46 (SiO_2). Their thicknesses were 30, 2, and 16 nm, respectively. The ellipsometry data for sample B are also well represented by a three-layer model with refractive indices of 1.96, 1.59, and 1.46, and layer thicknesses of 30, 4, and 4 nm, respectively. Refractive indices of 1.59–1.62 are intermediate between those of HfO_2 and SiO_2. It is, therefore, reasonable to assume that the intermediate layer either has a nonequilibrium structure and a composition of $Hf_xSi_yO_z$, which gradually varies from HfO_2 to $HfSiO_4$, or consists of a fine-particle two-phase mixture. Note that the thicknesses of the intermediate layer evaluated from cross-sectional TEM micrographs and ellipsometry data agree well.

XPS analysis. The chemical structure of the films was studied by XPS. An XPS survey scan of the surface of film A (Fig. 4) showed well-defined Hf, O, and C peaks. Carbon resided predominantly in the surface layer: ion milling for just 1 min sharply reduced its concentration. Thus, we are led to conclude that the carbon contamination of the surface resulted from exposure to the ambient atmosphere.

Figures 5 and 6 show the Hf 4*f*, Si 2*p*, and O1*s* XPS scans of films A and B, respectively, at different steps of depth profiling: spectra *1* were measured on the surface of the as-deposited films, and spectra *6* were obtained after 20 min of ion milling (film–substrate interface). Spectra *2*–*5* were obtained after 1, 4, 7, and 10 min of ion milling.

The Hf 4*f* level is known to be spin–orbit split into two components: Hf $4f_{7/2}$ and Hf $4f_{5/2}$. Accordingly, the Hf 4*f* spectrum of the as-grown film surface shows two narrow peaks at 16.6 and 18.3 eV, arising from Hf^{4+} (Fig. 5a, spectrum *1*). The spin–orbital splitting (energy separation between the Hf $4f_{7/2}$ and Hf $4f_{5/2}$ levels) is 1.66 eV. The binding energies reported for HfO_2 in the literature lie in the range 16.3–17.1 eV [9–12]. As the interface is approached, the Hf 4*f* emission of both samples gradually shifts to higher binding energies: the Hf $4f_{7/2}$ peak shifts from 16.6 to 18.6 eV. According to Wilk et al. [13] and Kato et al. [14], the formation of hafnium silicates may shift the Hf $4f_{7/2}$ peak up to 19.7 eV, depending on stoichiometry. The doublet around 16 eV, in the Hf $4f_{7/2}$ region, corresponds to hafnium in structurally imperfect HfO_2, produced by the Ar^+ beam during ion milling. This binding energy is close to that reported by Suzer et al. [15] for hafnium suboxides. After 20 min of ion milling, we observed an Hf $4f_{7/2}$ doublet around 15 eV, corresponding to hafnium silicide [13].

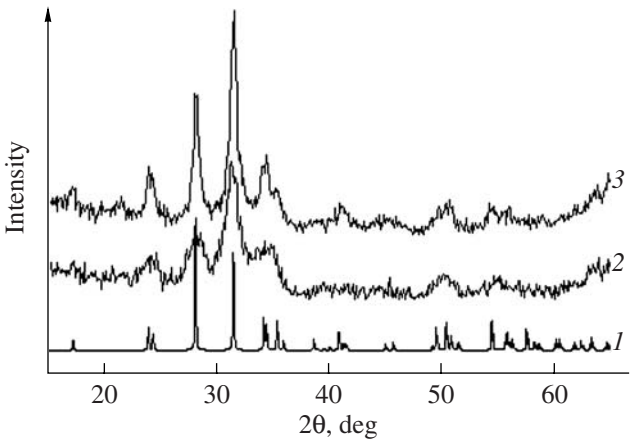

Fig. 3. XRD patterns of (*1*) monoclinic HfO_2 (PDF card 34-104), (*2*) HfO_2 film grown at 650°C, and (*3*) the same film after annealing at 800°C for 5 min.

Figure 5b illustrates the evolution of the Si 2*p* emission of sample A. The surface layer of the as-deposited film, as well as that after milling for 1 and 4 min (spectra *1*–*3*), was free of silicon. Further milling gave rise to a triplet in the Si 2*p* region, with maxima at 99.3, 101–102, and ≃104 eV. The 99.3-eV emission corresponds to unoxidized silicon, Si^0. The peak centered at ≃104 eV is obviously due to the Si^{4+} (oxidized silicon) in SiO_2 [14]. The weak, broad feature at 101–102 eV corresponds to hafnium silicates [14]. With increasing depth (spectra *4*, *5*), the Si^0 peak becomes stronger, while the Si^{4+} peak weakens. Spectrum *6* shows only the 99.3-eV peak, which corresponds to nearly complete removal of the film. The Si 2*p* binding energy in hafnium silicide is close to that in silicon [9]. It is, therefore, reasonable to

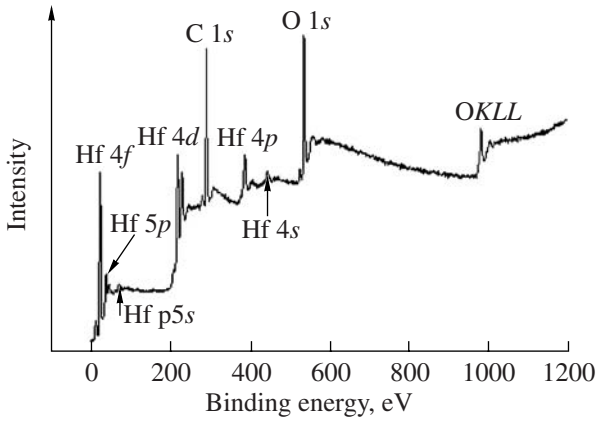

Fig. 4. Typical XPS survey scan of as-grown film.

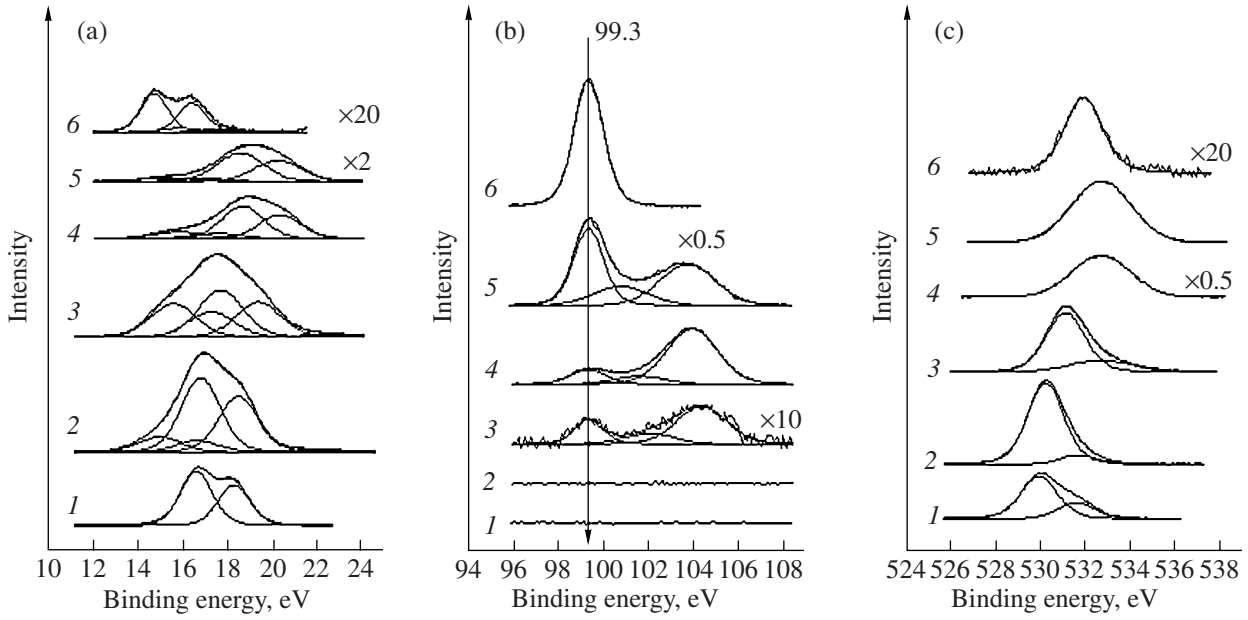

Fig. 5. (a) Hf 4*f*, (b) Si 2*p*, and (c) O 1*s* spectra obtained during depth profiling of an HfO_2 film grown at 650°C on a preoxidized (d_{SiO_2} = 20 nm) silicon substrate.

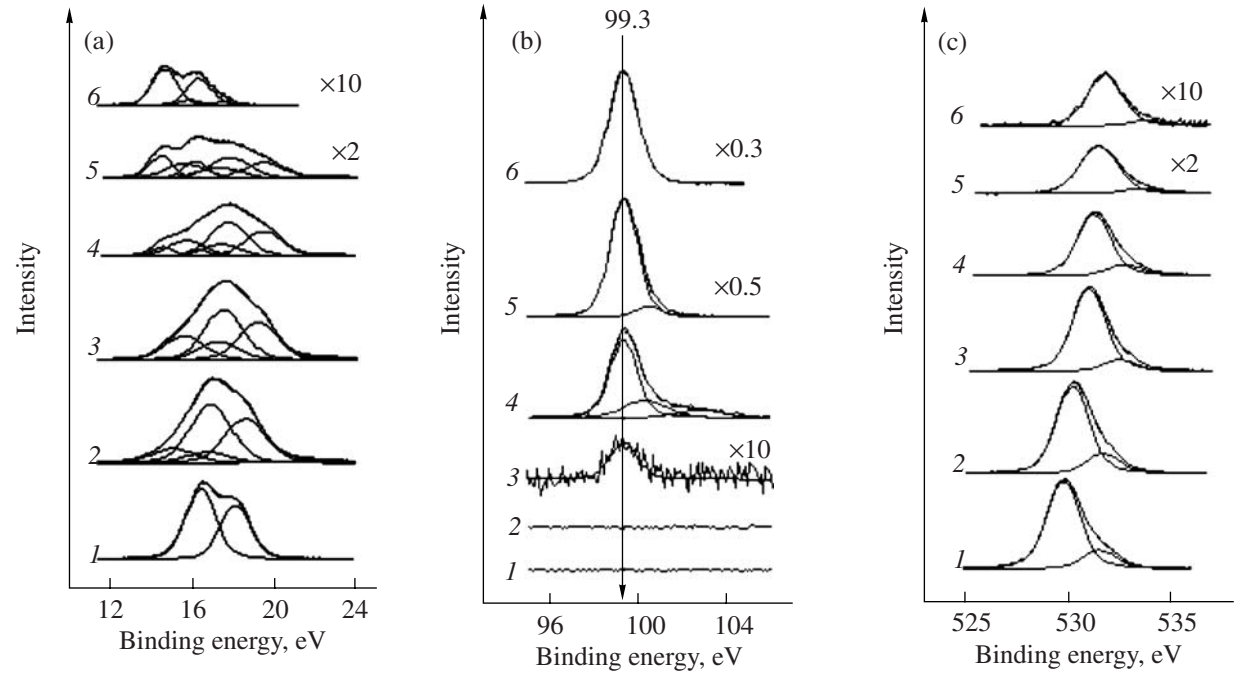

Fig. 6. (a) Hf 4*f*, (b) Si 2*p*, and (c) O 1*s* spectra obtained during depth profiling of an HfO_2 film grown on a silicon substrate with an oxide layer (d_{SiO_2} = 5 nm).

assume that the peak in question is due to the Si^0 and Si^{4+} in hafnium silicide.

During ion milling, the O 1*s* peak of sample A shifts rather sharply from 530 eV (characteristic of oxygen in HfO_2) to higher binding energies (Fig. 5c). In spectra *4* and *5*, the O 1*s* peak of sample A is located at 532.7 eV, which is characteristic of oxygen in SiO_2 [14]. Note that the corresponding Si 2*p* spectra show a strong peak near

104 eV, which is also attributable to SiO_2. Therefore, the silica layer in samples A (d_{SiO_2} = 20 nm) remains essentially intact, in good agreement with ellipsometry data. At the same time, the Si 2*p* spectrum shows a peak in the range 101–102 eV (silicon in hafnium silicates). Consequently, there is an intermediate layer 10–15 nm thick between the HfO_2 film and silicon substrate, which consists of a hafnium silicate and silica.

On the whole, the XPS spectrum of sample B varies in a similar manner in the course of ion milling (Fig. 6), but there are a number of distinctive features. Spectra *1–3* in Fig. 6a (Hf 4*f*) are similar to those of sample A. Spectra *4–6* in Fig. 6a show a prominent shoulder on the low-energy side, attributable to hafnium silicide [13]. A similar doublet, with an Hf $4f_{7/2}$ binding energy of 14.6 eV, only appeared in the spectrum of sample A after 20 min of ion milling (spectrum *6*). As pointed out in an earlier study [16], hafnium silicide may form through hafnium diffusion into the silicon resulting from oxygen removal during argon ion milling of the film. The most marked differences were observed between the Si 2*p* spectra of samples A and B. In the spectrum of sample B, the features characteristic of silicon in SiO_2 were missing. In particular, the spectrum taken after 7 min of ion milling showed, in addition to a sharp peak near 99.3 eV, weak features at 100.3 and 102.7 eV. Their position, however, corresponded to hafnium silicates [14]. During ion milling, the O 1*s* binding energy gradually increased from 530 to 531.5 eV, indicating that the chemical composition of the film gradually varied from HfO_2 on the film surface to $HfSi_xO_y$ at the HfO_2/Si interface. A similar shift of the O 1*s* peak was reported for $Hf_xSi_{1-x}O_y$ samples with x = 0–1 [14]. Thus, analysis of our XPS, ellipsometry, and electron microscopy data indicates that, during HfO_2 film growth, the silica layer reacts with the HfO_2 deposit. The Si–O bonds in the thin SiO_2 layer convert to Hf–O–Si bonds, with the formation of an intermediate layer. In sample A, having a thick (20 nm) pregrown SiO_2 layer, a hafnium silicate layer forms between the silica and hafnia layers, and only a part of the SiO_2 layer converts to the silicate. In sample B, in which the thickness of the native oxide layer is ≃5 nm, an intermediate layer of a nonstoichiometric hafnium silicate forms.

Thermodynamic analysis. Consider the present results from the thermodynamic point of view. To this end, it is convenient to use the isothermal section of the Si–SiO_2–HfO_2–Hf phase diagram at the temperature of hafnia deposition onto silicon (Fig. 7). This section has not been constructed previously using experimental data or thermodynamic calculations. To resolve this problem, we rely on phase-diagram data for the constituent binary systems and experimental data on the phase equilibria in the Si–Hf–O system. The Si–Hf system is known to contain the refractory silicides Hf_2Si, Hf_5Si_3 (stable only at high temperatures), Hf_3Si_2, HfSi, and $HfSi_2$ [17]. α-Hf, stable at 650°C, readily absorbs oxygen: the solid-solution range of HfO_x extends to $HfO_{0.206}$. The low-temperature form of hafnium oxide, HfO_{2-y}, exists in a rather broad range of oxygen stoichiometries: from ≃62 at % O to the stoichiometric composition HfO_2 [18, 19]. In the Si–O system at $p_{O_2} = 0.21 \times 10^5$ Pa, SiO_2 is the only oxide [19]. In the HfO_2–SiO_2 system, only one hafnium silicate has been identified: $HfSiO_4$ [20].

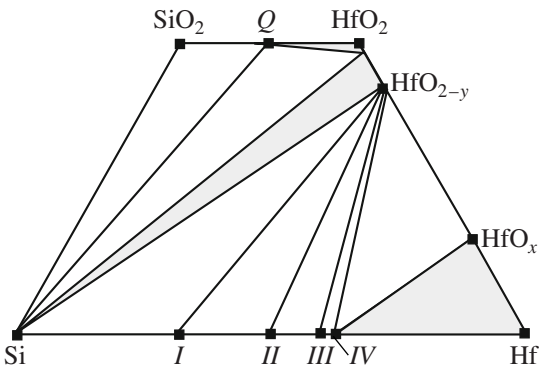

Fig. 7. Isothermal section of the Si–SiO_2–HfO_2–Hf phase diagram at the temperature of HfO_2 film growth on silicon (650°C); Q = $HfSiO_4$, I = Hf_2Si, II = Hf_3Si_2, III = HfSi, IV = $HfSi_2$; two-phase regions are marked by gray.

Using this information, one can construct all possible phase compatibility diagrams of the system under consideration, but additional data are needed to identify the proper diagram. In a number of studies [13, 21–25], the Si/HfO_2 system was concluded to be stable based on thermodynamic calculations. That conclusion, however, cannot be considered final because the problem was not completely defined. Indeed, to identify the proper phase compatibility diagram among the 28 possible, one must take into consideration all of the compounds existing in the system. In the calculations in question, only two intermetallic phases were taken into account, HfSi and $HfSi_2$, while the other hafnium silicides were left out of consideration. More direct evidence is provided by experimental data on the growth of HfO_2 films on silicon [4, 9, 16], which demonstrate that the Si/HfO_2 system is thermodynamically stable. This result uniquely defines the phase compatibility diagram of the Si–SiO_2–HfO_2–Hf system (Fig. 7). In the two-phase regions in Fig. 7, the HfO_x and HfO_{2-y} solid solutions coexist with stoichiometric compounds. The position of the tie lines in these regions depends on the oxygen pressure in the system. At low oxygen pressures, the tie line lies within the Si–HfO_{2-y} region. At a certain pressure, the HfO_2–Si equilibrium gives way to the HfO_2–$HfSiO_4$ equilibrium, and the Si/HfO_{2-y} system becomes unstable. The thermodynamically stable phase assemblage is then Si/$HfSiO_4$/HfO_{2-y}. The value of y depends on the oxygen partial pressure in the gas phase in contact with the film–substrate system. The

presence of a thin oxide film on the silicon surface is equivalent to a local increase in oxygen pressure and must, therefore, lead to the formation of a hafnium silicate layer.

CONCLUSIONS

The present ellipsometry, electron microscopy, and XPS data demonstrate that, during HfO_2 film growth on silicon, the native oxide reacts with the HfO_2 deposit to form an amorphous intermediate layer. Its refractive index of $\simeq$1.6, and its composition can be represented by $Hf_xSi_{1-x}O_y$.

Thermodynamic analysis of the Si–SiO_2–HfO_2–Hf system indicates that Si is in equilibrium with Si/HfO_{2-y} only at low oxygen pressures. Starting at a certain oxygen pressure (equivalent to the formation of a native oxide layer), the equilibrium phase assemblage is $Si/HfSiO_4/HfO_{2-y}$. Thus, the conclusions drawn from thermodynamic analysis are consistent with our experimental data.

ACKNOWLEDGMENTS

We are grateful to V.S. Danilovich and Yu.V. Shubin for the SEM and XRD measurements, respectively.

This work was supported by the Russian Foundation for Basic Research (project no. 05-03-32-393a), the Siberian Division of the Russian Academy of Sciences (integrated project no. 97), and the President's Grants Council for Support to Leading Scientific Schools (grant no. 636.2008.3).

REFERENCES

1. Packan, P.A., Pushing the Limits, *Science*, 1999, vol. 285, no. 5436, pp. 2079–2082.
2. Buchanan, D.A. and Lo, S.-H., Reliability and Integration of Ultra-thin Gate Dielectrics for Advanced CMOS, *Microelectron. Eng.*, 1997, vol. 36, p. 13.
3. Robertson, J., High Dielectric Constant Oxides, *Eur. Phys. J. Appl. Phys.*, 2004, vol. 28, pp. 265–291.
4. Yakovkina, L.V., Kichai, V.N., Smirnova, T.P., et al., Preparation and Properties of Thin HfO_2 Films, *Neorg. Mater.*, 2005, vol. 41, no. 12, pp. 1474–1479 [*Inorg. Mater.* (Engl. Transl.), vol. 41, no. 12, pp. 1300–1304].
5. *Handbook of X-ray Photoelectron Spectroscopy*, Wagner, C.D. et al., Eds., Muilenberg: Perkin-Elmer, 1978.
6. *ICDD/JCPDS Database of Crystallographic Data*, www.icdd.com.
7. Aarik, J., Aidla, A., Kiisler, A.-A., et al., Influence of Substrate Temperature on Atomic Layer Growth and Properties of HfO_2 Thin Films, *Thin Solid Films*, 1999, vol. 340, pp. 110–116.
8. Giannuzzi, L.A. and Stevie, F.A., A Review of Focused Ion Beam Milling Techniques for TEM Specimen Preparation, *Micron*, 1999, vol. 30, pp. 197–204.
9. Cho, M.-H., Roh, Y.S., Whang, C.N., et al., Thermal Stability and Structural Characteristics of HfO_2 Films on Si(100) Grown by Atomic Layer Deposition, *Appl. Phys. Lett.*, 2002, vol. 81, no. 3, pp. 472–474.
10. Renault, O., Samour, D., Damlencourt, J.-F., et al., HfO_2/SiO_2 Interface Chemistry Studied by Synchrotron Radiation X-ray Photoelectron Spectroscopy, *Appl. Phys. Lett.*, 2002, vol. 81, no. 19, pp. 3627–3629.
11. Sha, L., Puthenkovilakam, R., Lin, Y.-S., and Chang, J.P., Ion-Enhanced Chemical Etching of HfO_2 for Integration in Metal–Oxide–Semiconductor Field Effect Transistors, *J. Vac. Sci. Technol., B*, 2003, vol. 21, no. 6, pp. 2420–2427.
12. Fang, Q., Zhang, J.-Y., Wang, Z., et al., Interface of Ultrathin HfO_2 Films Deposited by UV-Photo-CVD, *Thin Solid Films*, 2004, vol. 453–454, pp. 203–207.
13. Wilk, G.D., Wallace, R.M., and Anthony, J.M., Hafnium and Zirconium Silicates for Advanced Gate Dielectrics, *J. Appl. Phys.*, 2000, vol. 87, pp. 484–492.
14. Kato, H., Nango, T., Miyagawa, T., et al., Plasma-Enhanced Chemical Vapor Deposition and Characterization of High-Permittivity Hafnium and Zirconium Silicate Films, *J. Appl. Phys.*, 2002, vol. 92, pp. 1106–1111.
15. Suzer, S., Sayan, S., Banaszak Holl, M.M., et al., Soft X-ray Photoemission Studies of Hf Oxidation, *J. Vac. Sci. Technol., A*, 2003, vol. 21, pp. 106–109.
16. Lee, J.-H., Ternary Phase Analysis of Interfacial Silicates Grown in HfO_x/Si and $HfO_x/SiO_2/Si$ Systems, *Thin Solid Films*, 2005, vol. 472, pp. 317–322.
17. Vol, A.E., *Stroenie i svoistva dvoinykh metallicheskikh sistem* (Structure and Properties of Binary Metallic Systems), Moscow: Fizmatgiz, 1962, vol. 2.
18. Rudy, E. and Stecher, P., Contribution to the Constitution of the System Hafnium–Oxygen, *J. Less-Common Met.*, 1963, vol. 5, p. 78.
19. Domagala, R.F. and Ruh, R., The Hafnium–Oxygen System, *Am. Soc. Met. Trans. Q.*, 1965, vol. 58, no. 2, p. 164.
20. Toropov, N.A., Barzakovskii, V.P., Bondar', I.A., and Udalov, Yu.P., *Diagrammy sostoyaniya silikatnykh sistem. Spravochnik* (Phase Diagrams of Silicate Systems: A Handbook), Leningrad: Nauka, 1969.
21. Ageeva, D.L., Phase Diagrams of Nonmetallic Systems, *Itogi Nauki*, 1966, no. 1.
22. Beyers, R., Thermodynamic Considerations in Refractory Metal–Silicon–Oxygen Systems, *J. Appl. Phys.*, 1984, vol. 56, no. 1, pp. 147–152.
23. Hubbard, K.J. and Schlom, D.C., Thermodynamic Stability of Binary Oxides in Contact with Silicon, *J. Mater. Res.*, 1996, vol. 11, pp. 2757–2776.
24. Gutowski, M., Jaffe, J.E., Liu, C.-L., et al., Thermodynamic Stability of High-*K* Dielectric Metal Oxides ZrO_2 and HfO_2 in Contact with Si and SiO_2, *Appl. Phys. Lett.*, 2002, vol. 80, no. 11, pp. 1897–1899.
25. Navrotsky, A., Thermochemical Insights into Refractory Ceramic Materials Based on Oxides with Large Tetravalent Cations, *J. Mater. Chem.*, 2005, vol. 15, pp. 1883–1890.